NARROW-BAND FEEDBACK SYSTEM TO DAMP TRANSVERSE COHERENT OSCILLATIONS OF BEAM IN THE U70

O. Lebedev, S. Ivanov, N. Ignashin, S. Sytov

Institute for High Energy Physics (IHEP), Protvino, Moscow Region, 142281, Russia

Abstract

Resistive-wall transverse coherent instability shows up as a major adverse factor in running the U70 proton synchrotron of IHEP-Protvino. The 10th azimuthal spatial harmonic of coherent beam perturbation is the worst one prone to a strong instability. To damp this particular beam mode selectively, a dedicated narrow-band feedback circuit has been developed. All of its hardware (comprising beam pickup and kicker plus analogue processing electronics) is housed in one and the same straight section of the ring lattice, the feedback circuit configuration thus being the local one. Such a straightforward layout minimizes inherent time delays and eases closing the two feedback loops servicing horizontal and vertical directions. The paper contains a brief technical specification of the damping system. Experimental results acquired during its turning on and beam-testing are outlined.

GENERALITIES

The transverse feedback in question is the so-called Local Feed-Back (LFB) system since all its essential components (beam pickup, HV electrostatic kicker, high-power and low-level processing electronics) are housed closely in the same period #2 of the U70 magnet lattice.

All the advantages of such a localized layout were routinely used for years for a base-band cancellation of a resistive wall impedance of a thin corrugated vacuum chamber in the U70 [1], rather than to impose damping per se. Still, in course of the machine upgrade, the thin-wall chamber was eventually replaced by a thick-wall smooth one. It hampered the prescribed operation of the feedback because frequency (f) dependence of transverse resistive-wall impedance no longer followed the transfer function vs. f through the open-loop feedback electronics.
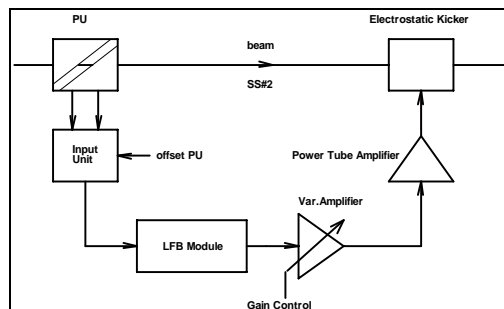

Figure 1: Block diagram of the LFB, a channel.

To this end, it was decided to revisit the low-level signal processing unit so as to impose strong damping to the azimuthal harmonic $k = -10$ of beam coherent perturbation. Its unstable frequency line $(k + Q)f_0$ is down-sampled to a vicinity of the DC, where Q is betatron tune,

$Q = 9.8$–9.9 in the U70; f_0 is rotation frequency; and the upper-sideband convention is used. To get a cost-effective solution, the high-power part of the circuit was left intact and two channels servicing horizontal (H) and vertical (V) directions were made identical.

HARDWARE

Block diagram of the LFB system is shown in Fig. 1. Beam-position sensor and actuator (beam kicker) are both the electrostatic (ES) plates.
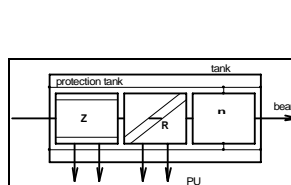

Figure 2: Station of ES beam-pickups, schematic view (left) and assembly in the lattice period #2 of U70 (right).

Schematic view of an askew-cut ES beam-pickup station and its outside appearance in the ring hall are shown in Fig. 2. Inner view of the station is disclosed by Fig. 3.

Figure 3: Station of ES beam-pickups, contents of the assembly box (left) and view along beam axis (right).

Table 1: Performance data of ES pickups

Plate capacitance, H/V	109.7 / 107.5	pF
Offset of electrical centre	–2 / +1	mm
Resonant frequency	60	MHz
Slope Δ/Σ, H/V	0.083 / 0.180	1/cm
Sensitivity Σ/Vgen @ 6 MHz	0.14	

Table 2: Performance data of ES kickers and amplifier

Length of plates along beam	1.3	m
Plate-to-plate gap, H/V	20 / 14	cm
Max voltage across gap	6	kV
Bandwidth @ –3 dB	0.5–400	kHz
Input resistance of amplifier	100	Ohm
Max input voltage, peak-to-peak	300	mV
In-out voltage gain	86	dB
Max attenuation via control circuit	–75	dB

Electrical circuit data of pickups and kickers is listed in Tables 1 and 2.

Outer view of ES kicker with its power amplifier and their observed amplitude-frequency transfer function are shown in Fig. 4.
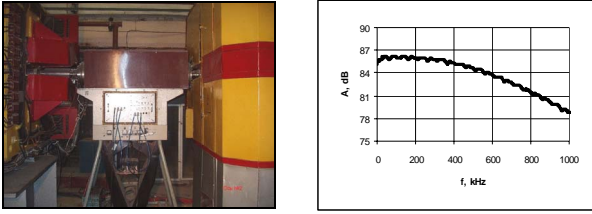

Figure 4: ES kicker with its power amplifier (left) and their amplitude–frequency transfer function (right).

Each channel of the LFB loop has a dedicated front-end input unit whose job is to monitor H/V beam position at SS #2 of the lattice and match pickup plate impedance to a characteristic wave impedance of a cable line that transports signal further to front-end electronics. Performance data is specified in Table 3.

Table 3: Performance data of an input unit

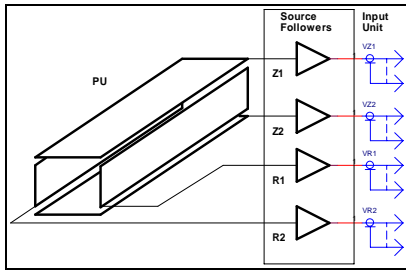| Bandwidth @ –3 dB	0.5 kHz – 17 MHz
In-out gain	about 0.8
Max amplitude of signal transferred to a 100 Ohm load	5 V
Protection interlock against beam loss at plates	available

Figure 5: Block diagram of input unit.

Block diagram of the input unit is shown in Fig. 5, its electrical circuit diagram being drawn in Fig. 6. Four source-follower amplifiers service each plate separately. Sum and difference signals are derived in a front-end electronic section. Overall transfer function is plotted in Fig. 7.
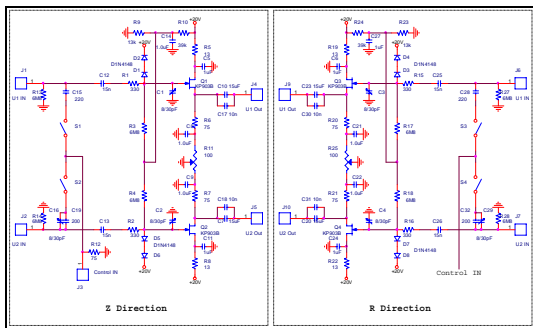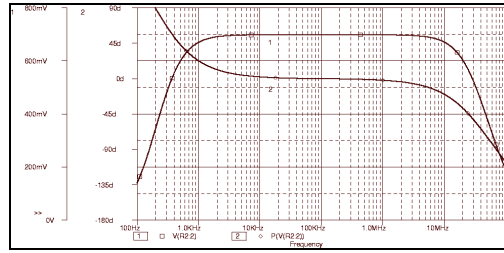

Figure 6: Electrical circuit of input unit.

Figure 7: Amplitude-frequency (*1*) phase-frequency (*2*) transfer function of an input unit with a front-end electronics. Electrical circuit modeling.

Fig. 8 shows equivalent circuit diagram of the open-loop LFB circuit as used for electrical circuit modeling. There are four functional parts outlined — a beam position monitor, an input unit, a core signal processing unit, and an ES beam kicker.
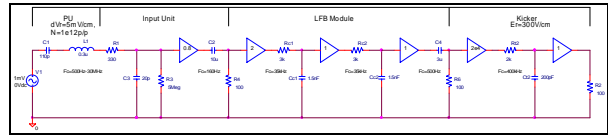

Figure 8: Start-to-end electrical equivalent circuit diagram of the open-loop LFB.

The circuit core constitutes a cascade connection of two identical integrating circuits with cutoff frequency $f_{CO} = $ 35 kHz (@ –3 dB) at which frequency the prescribed $\pi/2$-phase shift is attained. f_{CO} is set equal to anticipated central frequency of a typical operational span of a low-pass side-band $|k + Q|f_0$, $k = -10$, with possible variations of a working point Q and rotational frequency $f_0 = $ 183.7–202.0 kHz through cycle both taken into account.

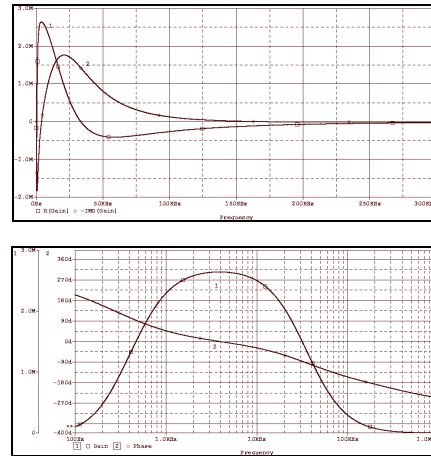Transfer functions of the circuit are plotted in Fig. 9.

Figure 9: Real (*1*) and imaginary (*2*) parts of transfer function (top). Amplitude- and phase-frequency transfer functions (bottom).

Horizontally, frequency line $|k + Q_H|f_0$ occurs within 14.7 – 72.3 kHz. Therefore, gain in amplitude varies by a factor of 4, while phase deviation staying within safe $\pm\pi/4$

w. r. t. a $\pi/2$-optimum. Suppression factor of the next rotational harmonic signal at $+f_0$ is around 20.

Vertically, the situation is eased by a narrower frequency span $|k + Q_V|f_0 = 29.4 – 43.2$ kHz allowing to use vertical LFB channel identical to the horizontal one.

Block diagram of a unified H/V feedback channel is shown in Fig. 10.

To ensure control over unwanted interference of a signal at a higher harmonic of rotational frequency, the amplifiers have got a remote gain control. To this end, a dedicated controller is installed locally in the ring hall of the U70. It acquires a series-code control signal transmitted via a cable route from the U70 main control console hall. Such a straightforward layout allows exercising control over two transverse directions with a single RF cable. In-out gain of the LFB is set with dedicated amplifier-attenuator within a range of –20 to +40 dB.

Outer view of electronic boards manufactured anew and installed is shown in Fig. 11.
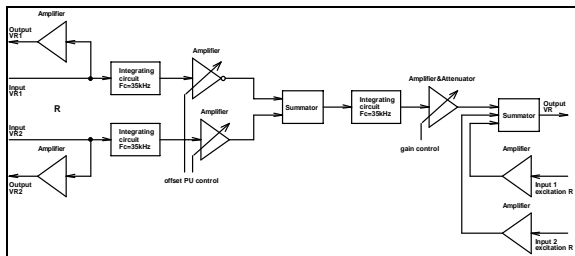

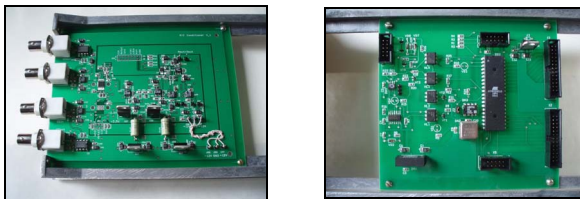Figure 10: Block diagram of LFB electronics.

Figure 11: Electronics of the LFB circuit (left) and local controller (right).

All the hardware parts of the LFB in question are mounted in the ring hall of the U70 near SS #2, as shown Fig. 12. The only exclusion constitutes electronics for a remote control, based on an industrial PC ROBO-2000 that is housed in the U70 main control console hall.

Figure 12: Shelf with a low-level electronics near SS #2 in ring hall of the U70.

STUDIES WITH BEAM

During the autumn (2007) run of the accelerator complex U70 of IHEP-Protvino, the narrow-band local transverse damping system was successfully put into test operation.

Fig. 13 presents experimental oscillograms observed. Left plot refers to a natural decay of betatron oscillations at injection flat bottom occurring due to de-coherence. Right plot shows effect of closing the feedback loop. Extra damping factor due to the feedback is around 100 w. r. t. the natural decay time.
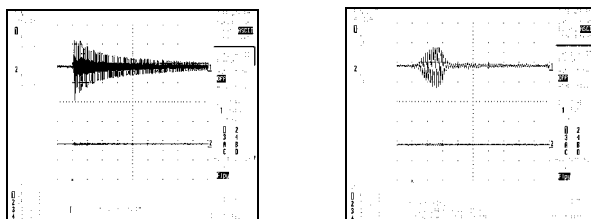

Figure 13: Natural damping of betatron oscillations due to de-coherence, LFB is off, decay time = 30 ms (left). Damping with LFB on, decay time = 250 µs (right).

In a routine operation of the U70, patterns of its orbit filling with bunches are, more often than not, non-symmetric. Bunch-to-bunch eigenmodes for such a beam are not obliged to be orthogonal to the 10th azimuthal harmonic of coherent beam perturbation. Therefore, the narrow-band low-pass feedback in question was found to see and dampen out a wider scope of coupled-bunch modes. In this respect, its observed stabilizing effect has exceeded our expectations.

CONCLUSION

Upgrading and successful test operation of the local narrow-band transverse beam feedback in the U70 constituted a noticeable step towards improving beam quality by keeping lower values of beam transverse emittances on the injection flat bottom and making the beam less susceptible to external deflecting interferences through a magnet cycle of the machine.

Further plans along this direction foresee gradual upgrade of the wide-band transverse beam feedback in the U70 by going to a DSP electronics to cope with varying time delays required.

REFERENCES

[1] V. Balbekov, K. Gertsev, O. Lebedev, Damping Systems of Beam Transverse Dipole Oscillations in IHEP Accelerator, Preprint IHEP 84–23, Serpukhov, 1984.